Technical Notes and Correspondence

Stochastic Robustness of Linear Time-Invariant Control Systems

Robert F. Stengel and Laura R. Ray

Abstract—**A simple numerical procedure for estimating the *stochastic robustness* of a linear time-invariant system is described. Monte Carlo evaluation of the system's eigenvalues allows the *probability of instability* and the related *stochastic root locus* to be estimated. This analysis approach treats not only Gaussian parameter uncertainties but non-Gaussian cases, including uncertain-but-bounded variations. Confidence intervals for the scalar probability of instability address computational issues inherent in Monte Carlo simulation. Trivial extensions of the procedure admit consideration of alternate discriminants; thus, the probabilities that stipulated degrees of instability will be exceeded or that closed-loop roots will leave desirable regions can also be estimated. Results are particularly amenable to graphical presentation.**

I. Introduction

Control system robustness is defined as the ability to maintain satisfactory stability or performance characteristics in the presence of all conceivable system parameter variations. While assured robustness may be viewed as an alternative to gain adaptation or scheduling to accommodate known parameter variations, more often it is seen as protection against uncertainties in plant specification. Consequently, a statistical description of control system robustness is consistent with what may be known about the structure and parameters of the plant's dynamic model.

Guaranteeing robustness has long been a design objective of control system analysis, although in most instances, insensitivity to parameter variations has been treated as a deterministic problem (see [1] for a comprehensive presentation of both classical and modern robust control). Stability (gain and phase) margins are useful concepts for designing robust single-input/single-output systems, addressing disturbance rejection and other performance goals, and they are amenable to the manual graphical procedures that preceded the widespread use of computers. With the help of computers, singular-value analysis has extended the frequency-domain approach to multiinput/multioutput systems (e.g., [2], [3]); however, guaranteed stability-bound estimates often are unduly conservative, and the relationship to parameter variations in the physical system is weak. Structured singular-value analysis [4] reduces this conservatism somewhat, and alternate treatments of structured parameter variations have been proposed (e.g., [5]–[7]), although these approaches remain deterministic. Reference [8] uses the term "stochastic robustness" to describe a stability bound based on Lyapunov methods and parameter perturbations that are modeled as stochastic sequences. This is a deterministic stability bound expressed in terms of the norm of a vector of noise variances. Elements of "stochastic stability" [9] have application to robustness but have yet to be presented in that context.

The notion of *probability of instability*, which is central to the analysis of stochastic robustness, was introduced in [10], with application to the robustness of the Space Shuttle's flight control system, and it is further described in [11]–[14]. This method determines the *stochastic robustness* of a linear time-invariant system by the probability distributions of closed-loop eigenvalues, given the statistics of the variable parameters in the plant's dynamic model. The probability that all of these eigenvalues lie in the open left-half s plane is the scalar measure of robustness.

With the advent of graphics workstations, the stochastic robustness of a system is easily computed by Monte Carlo simulation, and results can be displayed pictorially, providing insight into otherwise hidden robustness properties of the system. The method is computationally simple, requiring only matrix manipulation and eigenvalue computation, and it is inherently nonconservative, given a large enough sample space. Furthermore, the analysis of stochastic robustness is a logical adjunct to parameter-space control design methods [15]–[18]. Details of the approach and an example are given in the sequel.

Manuscript received October 14, 1988; revised September 30, 1989. Paper recommended by Associate Editor at Large, A. Benveniste. This work was supported by the FAA and the NASA Langley Research Center under Grant NGL 31-001-252.

The authors are with the Department of Mechanical and Aerospace Engineering, Princeton University, Princeton, NJ 08544.

IEEE Log Number 9039313.

II. Probability of Instability

Consider a linear time-invariant (LTI) system subject to LTI control

$$\dot{x}(t) = F(p)x(t) + G(p)u(t) \tag{1}$$

$$y(t) = H(p)x(t) \tag{2}$$

$$u(t) = u_c(t) - CH(p)x(t) \tag{3}$$

$x(t)$, $u(t)$, $y(t)$, and p are state, control, output, and parameter vectors of dimension n, m, q, and r, respectively, accompanied by conformable dynamic, control, and output matrices F, G, and H, which may be arbitrary functions of p. $u_c(t)$ is a command input vector, and, for simplicity, the $(m \times n)$ control gain matrix C is assumed to be known without error. The n eigenvalues, $\lambda_i = \sigma_i + j\omega_i$, $i = 1$ to n, of the matrix $[F(p) - G(p)CH(p)]$ determine closed-loop stability and can be determined as the roots of the determinant equation

$$|sI_n - [F(p) - G(p)CH(p)]| = 0 \tag{4}$$

where s is a complex operator and I_n is the $(n \times n)$ identity matrix. While the explicit relationship between parameters and eigenvalues is complicated, estimating the probability of instability of the closed-loop system from repeated eigenvalue calculation is a straightforward task. Putting aside the mathematical intricacies, note that the probability of stability plus the probability of instability is one. Since stability requires all the roots to be in the open left-half s plane, while instability results from even a single right-half s plane root, we may write

$$\Pr(\text{instability}) \triangleq \mathbb{P} = 1 - \int_{-\infty}^{0} \text{pr}(\sigma)\, d\sigma \tag{5}$$

where σ is an n-vector of the real parts of the system's eigenvalues ($\lambda = \sigma + j\omega$), $\text{pr}(\sigma)$ is the joint probability density function of σ (unknown analytically), and the integral that defines the probability of stability is evaluated over the space of individual components of σ. Denoting the probability density function of p as $\text{pr}(p)$, (4) is evaluated J times with each element of p_j, $j = 1$ to J, specified by a random-number generator whose individual outputs are shaped by $\text{pr}(p)$. This *Monte Carlo evaluation* of the probability of stability becomes increasingly precise as J becomes large. Then

$$\int_{-\infty}^{0} \text{pr}(\sigma)\, d\sigma = \lim_{J \to \infty} \frac{N(\sigma_{\max} \le 0)}{J}. \tag{6}$$

0018-9286/91/0100-0082$01.00

$N(\cdot)$ is the number of cases for which all elements of σ are less than or equal to zero, that is, for which $\sigma_{\max} \leq 0$, where $\sigma_{\max}$ is the maximum real eigenvalue component in σ. An important feature of this definition is that it does not depend on the eigenvalues and eigenvectors retaining fixed structures. As parameters change, complex roots may coalesce to become real roots (or the reverse), and modes may exchange relative frequencies. The only matter for concern is whether or not all real parts of the eigenvalues remain in the left-half s plane. For $J < \infty$, the probability of instability resulting from Monte Carlo evaluation is an estimate, denoted $\hat{\mathbb{P}}$.

Histograms and cumulative distributions for varying degrees of stability are readily given by the Monte Carlo estimate of $\int_{-\infty}^{\Sigma} \mathrm{pr}(\sigma)\, d\sigma$, where Σ represents a maximum real eigenvalue component, and $-\infty < \Sigma < \infty$. This histogram is a plot of $N[(\Sigma - \Delta) < \sigma_{\max} \leq \Sigma]/J$ versus Σ; Δ is an increment in Σ, $N[\cdot]$ is the number of cases whose maximum real eigenvalue components lie in the increment, and J is the total number of evaluations. The histogram estimates the *stability probability density function*, $\mathrm{pr}(\Sigma)$, which is obtained in the limit for a continuous distribution of Σ as $\Delta \to 0$ and $J \to \infty$. The *cumulative probability distribution of stability*, $\Pr(\Sigma)$, is similarly estimated and presented as $N(\sigma_{\max} \leq \Sigma)/J$ versus Σ, the exact distribution being achieved in the limit as $J \to \infty$. Consequently

$$\mathbb{P} = 1 - \Pr(0). \tag{7}$$

There is, of course, no limitation on admissible specifications for the multivariate $\mathrm{pr}(\boldsymbol{p})$; it may be Gaussian or non-Gaussian, as appropriate. Rayleigh, correlated, and any other well-posed distributions are admissible, the principal challenge being to properly shape (and correlate) the outputs of the random-number generator. In practice, system parameter uncertainties are most likely to be bounded, as typical quality control procedures eliminate out-of-tolerance devices, and there are physical limitations on component size, weight, shape, etc. The uniform distribution is particularly interesting, as it readily models bounded uncertainty, and it is the default distribution of most algorithms for random-number generation. Given binary distributions for each parameter, in which the elements of $\boldsymbol{p}$ take maximum or minimum values with equal probability, the Monte Carlo evaluation reduces to 2^r deterministic evaluations, the result is exact, and the probability associated with each possible value of $\boldsymbol{p}$ is $1/2^r$. Similarly, the distribution for r parameters, each of which takes w values (i.e., for quantized uniform distributions), can be obtained from w^r evaluations; the probability of acquiring each value of $\boldsymbol{p}$ is $1/w^r$.

When has stochastic robustness been achieved? The answer is problem-dependent. $\mathrm{pr}(\boldsymbol{p})$ should be chosen to reflect physical limits of parameter uncertainty. In some applications involving bounded parameters, it will be possible to choose $\boldsymbol{C}$ such that $\mathbb{P} = 0$, and that is a desirable goal; however, if admissible parameter variations are unbounded, if $\boldsymbol{C}$ is constrained, or if the rank of $\boldsymbol{CH}$ is less than n, the minimum $\mathbb{P}$ may be greater than zero. $\boldsymbol{C}$ then must be chosen to satisfy performance goals and one of two robustness criteria: minimum $\mathbb{P}$, or $\mathbb{P}$ small enough to meet a reliability specification (e.g., one chance of instability in some larger number of realizations). One may object that the parameter distributions must be known or estimated for stochastic robustness analysis. However, if robustness estimates are strongly dependent on the statistics, then it is incumbent on the designer to know something about the statistics. Otherwise, the final control system may be either unduly conservative (at the expense of performance) or insufficiently robust in the face of real-world uncertainties.

II. Stochastic Root Locus

While it is not necessary to plot the eigenvalues of (4) to determine or portray stochastic robustness, stochastic root loci provide insight regarding the effects of parameter uncertainty on system stability. Consider, for example, a classical second-order system with characteristic equation

$$s^2 + 2\zeta\omega_n s + \omega_n^2 = 0. \tag{8}$$

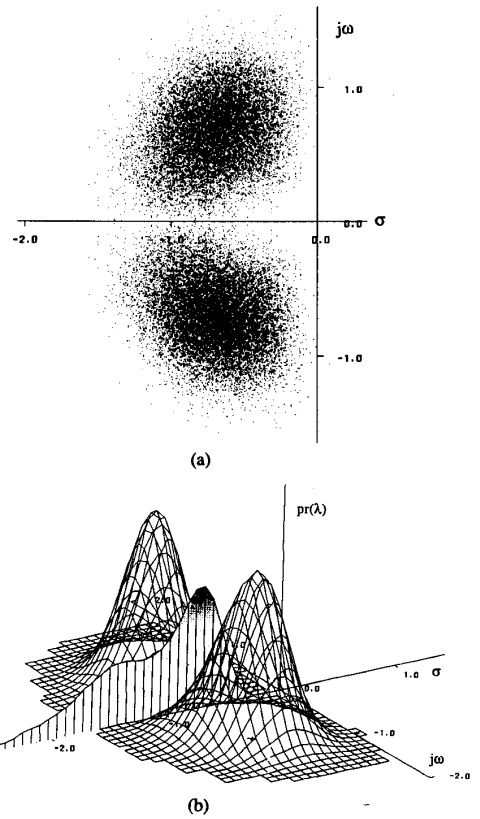

Fig. 1. Stochastic root loci of a second-order system with Gaussian damping ratio and natural frequency. $\zeta_0 = 0.707$, $\omega_{n0} = 1$; 50 000 Monte Carlo evaluations. The root density pr (λ) is given in units of roots/unit length along the real axis and roots/unit area in the complex plane. (a) Scatter plot. (b) Oblique three-dimensional representation.

Suppose that the damping ratio (ζ) and natural frequency (ω_n) are nominally 0.707 and 1, respectively, and that each may be a Gaussian-distributed random variable with standard deviation of 0.2. Root loci for individual parameter variations would follow classical configurations of root locus construction, with the heaviest density of roots in the vicinities of the nominal roots. If both ζ and ω_n are uncertain and uncorrelated (i.e., $\boldsymbol{p} = [\zeta\ \omega_n]^T$), the possible root locations become "clouds" surrounding the nominal values [Fig. 1(a)]. Understanding of robustness issues can be gained by plotting the density of the roots in a third dimension above the root locus plot [Fig. 1(b)]. This can be done by simply dividing the s plane into subspaces (or "bins") and counting the number of roots in each bin as a sampled estimate of the *root density* ρ. The result is a multivariate histogram, with σ and ω serving as independent variables. Complex root bins are elemental areas, for which ρ_A is defined in units of roots/unit area. Real root bins are confined to the real axis; hence, ρ_L measures roots/unit length. The density of roots depicts the likelihood that eigenvalues vary from their nominal values, including branches on the real axis and in the right-half s plane for large enough variations of ζ and ω_n. Fig. 1 is based on 50 000 Monte Carlo evaluations, and numerical smoothing has been applied to account for sampling effects. An example of the histogram and cumulative distribution is given in Fig. 2. The probability-of-instability estimate ($\Sigma = 0$ on the cumulative distribution) is 8×10^{-5}.

When considering instability, distinction must be made between the number of *cases* with right-half plane roots and the number of *roots* in the right-half plane. For example, a third-order system can be unstable with 1, 2, or 3 roots in the right-half plane, yet N

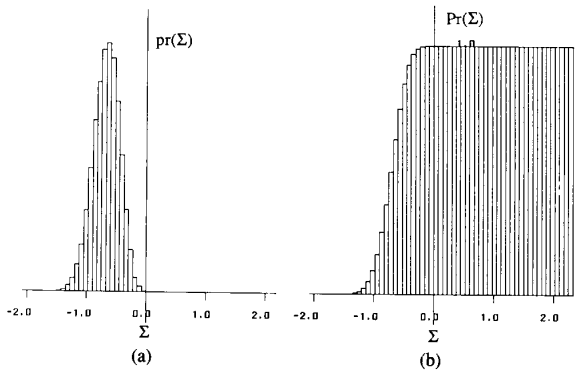

Fig. 2. (a) Histogram and (b) cumulative distribution for the second-order system with Gaussian damping ratio and natural frequency.

would be incremented by one in each case. A high-order system with real roots could be unstable with one or more roots in the same right-half plane bin. Again, N would be incremented by one, although the bin's ρ depends upon the number of roots it contains.

III. Confidence Intervals

Because it is an estimate, $\hat{\mathbb{P}}$ must have associated with it some notion of accuracy or relationship to the true underlying probability of instability $\mathbb{P}$. Confidence intervals relate $\hat{\mathbb{P}}$ to $\mathbb{P}$ by bounding the (unknown) true value with defined certainty. A confidence statement for $\mathbb{P}$ is

$$\Pr(L < \mathbb{P} < U) = 1 - \alpha \tag{9}$$

where (L, U) is the interval estimate (lower and upper bounds), $1 - \alpha$ is the confidence coefficient, and $\mathbb{P}$ lies within (L, U) with $100(1 - \alpha)\%$ confidence. Appropriate selection of the confidence coefficient and the number of evaluations determines the interval width.

The method used to compute confidence intervals depends on the underlying probability distribution of the variable in question. The probability of instability is a *binomial variable*, with the outcome of a trial taking one of two possible values (stable or unstable) for each Monte Carlo evaluation. $\mathbb{P}$ therefore has a binomial probability density and cumulative distribution given by

$$\text{pr}(x) = (J, x)\mathbb{P}^x(1 - \mathbb{P})^{J-x} \tag{10}$$

$$\Pr(X \le x) = \sum_{j \le x} (J, j)\mathbb{P}^j(1 - \mathbb{P})^{J-j} \tag{11}$$

where x is the number of occurrences of instability in J evaluations, and (J, x) is the binomial coefficient, $J!/x!(J - x)!$. The *binomial test* is applied to determine exact confidence intervals for binomial variables. The lower and upper confidence bounds are derived from the cumulative distribution and satisfy [19]

$$\Pr(X \le x - 1) = \sum_{j=0}^{x-1} (J, j)L^j(1 - L)^{J-j} = 1 - \frac{\alpha}{2} \tag{12}$$

$$\Pr(X \le x) = \sum_{j=0}^{x} (J, j)U^j(1 - U)^{J-j} = \frac{\alpha}{2} \tag{13}$$

where $1 - \alpha$ is the required confidence coefficient and X is the actual number of unstable cases after J evaluations ($X = J\hat{\mathbb{P}}$).

The validity of the Monte Carlo analysis depends on a number of simulation parameters: the number of eigenvalues computed, the number of varying parameters, and their probability distributions. However, by applying the binomial test, the derivation of explicit relationships between simulation parameters and the required number of evaluations is avoided. Nevertheless, it offers a rigorous theory by which to calculate exact confidence intervals. The number of evaluations required for a specified confidence interval can be related to a single variable, $\mathbb{P}$, and this relationship is valid for any simulation parameters or application.

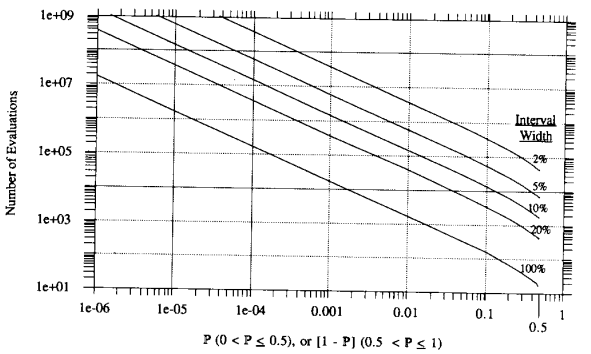

Fig. 3. Number of evaluations required for given confidence interval widths and confidence coefficient $1 - \alpha = 0.95$. Interval width is given as percent of $\mathbb{P}$. For $\mathbb{P} > 0.5$, the curves are symmetric, with the number of evaluations given by that for $1 - \mathbb{P}$.

Fig. 3 presents the number of evaluations required for specified interval widths and a 95% confidence coefficient, given as a percentage of $\mathbb{P}$. An estimate $\hat{\mathbb{P}}$ based on a small number of evaluations can be used as the abscissa of Fig. 3 to forecast the total number of evaluations required for the desired interval width. A larger confidence coefficient shifts the curves of Fig. 3 to higher numbers of evaluations.

IV. Stochastic Robustness Example

An example of the application of stochastic robustness is based on the longitudinal dynamics and control of an open-loop-unstable aircraft. The Forward-Swept-Wing Demonstrator's aerodynamic center is forward of its center of gravity, resulting in static instability. Its stability matrix, control-effect matrix, and open-loop eigenvalues are

$$\boldsymbol{F} = \begin{bmatrix} -0.02 & -0.3 & -0.4 & -32.2 \\ -0.0001 & -1.2 & 1 & 0 \\ 0 & 18. & -0.6 & 0 \\ 0 & 0 & 1 & 0 \end{bmatrix} \tag{14}$$

$$\boldsymbol{G} = \begin{bmatrix} -.04 & 35. \\ 0 & 0 \\ 0.2 & -0.2 \\ 0 & 0 \end{bmatrix} \tag{15}$$

$$\lambda_{1-4} = -0.1 \pm 0.057j, -5.15, 3.35. \tag{16}$$

The state components represent forward velocity, angle of attack, pitch rate, and pitch angle. The principal control surfaces are the canard control surface and the thrust setting. Possible uncertainties in aerodynamic and thrust effects as well as separate dynamic pressure (ρ and V) effects lead to a 12-element parameter vector (the remaining terms are kinematic, due to gravity, identically zero, or otherwise negligible)

$$\boldsymbol{p} = [\rho\, V f_{11} f_{12} f_{13} f_{22} f_{32} f_{33} g_{11} g_{12} g_{31} g_{32}]. \tag{17}$$

Although velocity (V) and air-density (ρ) are essentially deterministic, including them as parameters gives the ability to look at flight condition perturbations around the nominal value and reduces correlation of the remaining parameters. ρ and V are modeled as uniform parameters, giving an indication of stochastic robustness over a

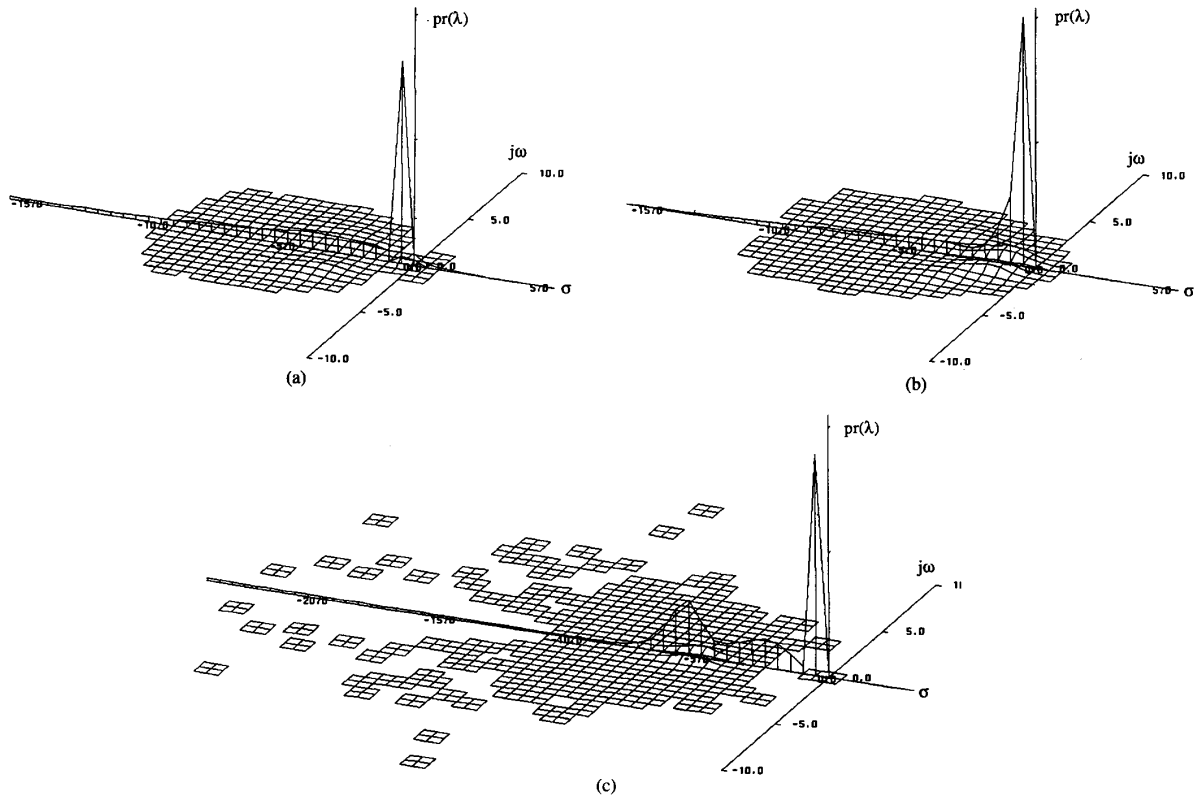

Fig. 4. Stochastic root loci for the Forward-Swept-Wing Demonstrator Aircraft with Gaussian parameters, Cases (a), (b), and (c). The root density pr (λ) is given in units of roots/unit length along the real axis and roots/unit area in the complex plane.

TABLE I
PARAMETERS FOR FORWARD-SWEPT-WING DEMONSTRATOR AIRCRAFT EXAMPLE

Case (a)	$C = \begin{bmatrix} 0.1714 & 130.26 & 33.165 & 0.364 \\ 0.984 & -11.387 & -2.968 & -1.133 \end{bmatrix}$	$Q = \text{diag}(1,1,1,0)$	$R = \text{diag}(1,1)$	$\lambda = -35.0, -5.14, -3.32, -0.0183$			
Case (b)	$C = \begin{bmatrix} 0.0270 & 82.659 & 20.927 & -0.0638 \\ 0.0107 & -62.623 & -16.203 & -1.902 \end{bmatrix}$	$Q = \text{diag}(1,1,1,0)$	$R = 1000\,\text{diag}(1,1)$	$\lambda = -5.15, -3.36, -1.09, -0.0186$			
Case (c)	$C = \begin{bmatrix} 0.1349 & 413.294 & 104.633 & -0.3191 \\ 0.0535 & -313.112 & -81.015 & -9.509 \end{bmatrix}$	$\lambda = -32.21, -5.15, -3.44, -0.01$					

range of flight conditions. In terms of the elements p, F, and G are

$$F = \begin{bmatrix} \dfrac{-2gf_{11}}{V} & \dfrac{\rho V^2 f_{12}}{2} & \rho V_{13} & -g \\ \dfrac{-45}{V^2} & \dfrac{\rho V f_{22}}{2} & 1 & 0 \\ 0 & \dfrac{\rho V^2 f_{32}}{2} & \rho V f_{33} & 0 \\ 0 & 0 & 1 & 0 \end{bmatrix}, \quad (18)$$

$$G = \frac{\rho V^2}{2}\begin{bmatrix} g_{11} & g_{12} \\ 0 & 0 \\ g_{31} & g_{32} \\ 0 & 0 \end{bmatrix}. \quad (19)$$

Linear-quadratic controllers are designed according to three specifications: (a) Q = diag (1, 1, 1, 0), R = diag (1, 1); (b) Q = diag (1, 1, 1, 0), R = diag (1000, 1000); and (c) the control gain matrix of Case (b) is multiplied by an arbitrary factor (5) to restore the closed-loop bandwidth to that of Case (a). The resulting control gain matrices and corresponding nominal closed-loop eigenvalues are given in Table I. These three cases have not been chosen to satisfy any particular performance criteria, but merely to demonstrate the impact of differing generalized design criteria on stochastic robustness. Furthermore, the designs are not meant to reflect acceptable control laws, as the high gains were purposely chosen to magnify robustness problems and to illustrate the application of stochastic robustness.

For illustration, ρ and V are $\pm 30\%$ uniform parameters, and the remaining elements of p are subject to independent 30% standard deviation Gaussian uncertainties. Fig. 4 shows the stochastic root loci for each case, based on 25 000 Monte Carlo evaluations. In each case, the eigenvalue near the origin is least affected by the parameter changes, and its peak dominates the distribution. In Cases (a) and (c), the eigenvalue farthest to the left (not shown in Fig. 4) has an enormous variance along the real axis. Interaction of roots

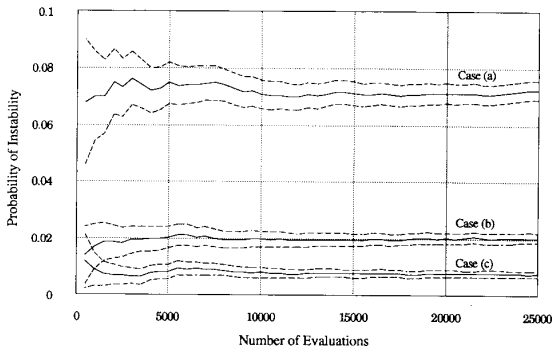

Fig. 5. 95% confidence intervals ($\alpha = 0.05$) based on the binomial test for the Forward-Swept-Wing Demonstrator Aircraft with Gaussian parameters, Cases (a), (b), and (c). Solid line represents $\hat{\mathbb{P}}$ estimate, and dashed lines give confidence intervals.

around the origin causes instability. The corresponding probability-of-instability estimates and 95% confidence intervals are (a) 0.0724 (0.0692, 0.0756), (b) 0.0205 (0.0187, 0.0222), and (c) 0.0076 (0.0065, 0.0086). Robustness improves from Case (a) to (b) as control usage is restrained by high control weighting, and the ad hoc robustness recovery technique used in Case (c) gives additional improvement. Fig. 5 shows 95% confidence intervals and the $\hat{\mathbb{P}}$ history with the number of evaluations. While confidence intervals for Cases (b) and (c) initially overlap, 25 000 evaluations are more than sufficient to rank the three cases in order of robustness.

For uniformly distributed parameters in $[0.7\boldsymbol{p}, 1.3\boldsymbol{p}]$, the extent of the parameter and eigenvalue distributions decreases substantially (Fig. 6). A comparison of Figs. 4 and 6 gives a better indication of the effects of Gaussian "tails" on the eigenvalue probability densities. $\hat{\mathbb{P}}$ and confidence intervals for 25 000 evaluations are (a) 3.6E-4 (1.25E-4, 5.95E-4) and (b) and (c) zero (0, 1.48E-4). For 12-parameter binary distributions, 4096 evaluations produce exact results. $\hat{\mathbb{P}}$ for each case is (a) 0.1191 and (b) and (c) zero.

Stochastic stability robustness is given as a function of the control design parameter ν, where the LQR control weighting matrix $\boldsymbol{R} = \nu \boldsymbol{I}_2$ (Fig. 7). Under the specified limits of parameter uncertainty, the distinction in stability and robustness versus design parameter statistics is apparent. Note that the qualitative result that $10 < \nu < 10^5$ provides the most robust designs is independent of the assumed probability distribution. In particular, the fact that the minimum-control-energy case ($\nu \to \infty$) represents the least robust design would not be obvious using standard robustness analysis techniques such as unstructured-singular-value analysis. While the exact relationship between parameter uncertainty and eigenvalue location is complicated, the increase in $\mathbb{P}$ beyond 10^5 is attributed to the shift in the closed-loop eigenvalues towards the imaginary axis. For example, at $\nu = 10^8$ the closed-loop eigenvalues are -5.15, -3.35, $-0.0104 \pm 0.057j$; the first two are almost identical to those of Case (b), while the complex pair is closer to the imaginary axis. The kind of results presented in Fig. 7 offer controller design insight and show nonobvious robustness characteristics.

V. Conclusion

Stochastic robustness offers a rigorous yet straightforward alternative to current metrics for control system robustness that is simple to compute and is unfettered by normally difficult problem statements, such as non-Gaussian statistics, products of parameter variations, and structured uncertainty. The approach answers the question, "How likely is the closed-loop system to fail, given limits of parameter uncertainty?" It makes good use of modern computational and graphic tools, and it is easily related to practical design considerations. The principal difficulty in applying this method to controlled systems is that it is computationally intensive; however, requirements are well within the capabilities of existing computers. The principal advantage of the approach is that it is easily implemented, and results have direct bearing on engineering objectives.

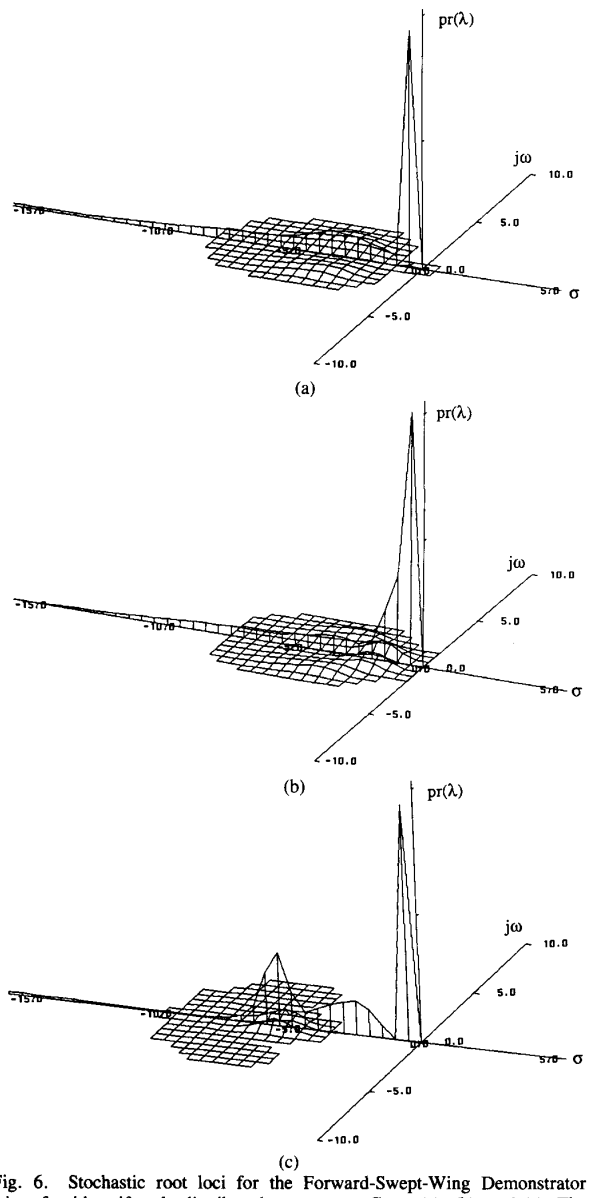

Fig. 6. Stochastic root loci for the Forward-Swept-Wing Demonstrator Aircraft with uniformly distributed parameters, Cases (a), (b), and (c). The root density pr (λ) is given in units of roots/unit length along the real axis and roots/unit area in the complex plane.

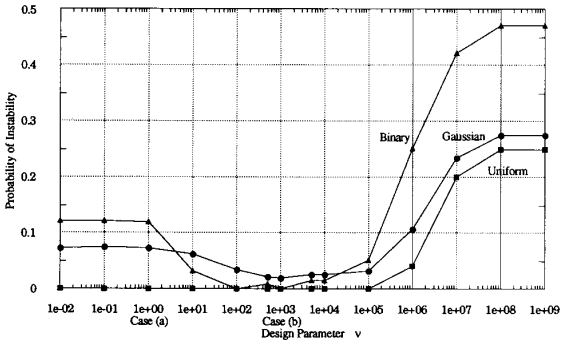

Fig. 7. Probability-of-instability estimates versus LQR design parameter ν ($\boldsymbol{R} = \nu \boldsymbol{I}_2$) for forward-swept wing aircraft example.

ACKNOWLEDGMENT

The authors are grateful to Prof. W. VanderVelde of M.I.T. for helpful discussions on this subject.

REFERENCES

[1] P. Dorato, Ed., *Robust Control*. New York: IEEE Press, 1987.
[2] N. R. Sandell, Jr., Ed., "Recent developments in the robustness theory of multivariable systems," Office of Naval Research, Rep. no. ONR-CR215-271-1F, Aug. 1979.
[3] N. A. Lehtomaki, N. R. Sandell, Jr., and M. Athans, "Robustness results in linear-quadratic-Gaussian-based multivariable control designs," *IEEE Trans. Automat. Contr.*, vol. AC-26, no. 1, pp. 75-93, Feb. 1981.
[4] J. C. Doyle, "Analysis of feedback systems with structured uncertainties," *IEE Proc.*, vol. 129, pt. D, no. 6, pp. 242-250, Nov. 1982.
[5] M. Tahk and J. L. Speyer, "Modeling of parameter variations and asymptotic LQG synthesis," *IEEE Trans. Automat. Contr.*, vol. AC-32, no. 9, pp. 793-801, Sept. 1987.
[6] R. K. Yedavalli and Z. Liang, "Reduced conservatism in stability robustness bounds by state transformation," *IEEE Trans. Automat. Contr.*, vol. AC-31, no. 9, pp. 863-866, Sept. 1986.
[7] I. Horowitz, "Quantitative feedback theory," *IEE Proc.*, vol. 129, pt. D, no. 6, pp. 215-226, Nov. 1982.
[8] E. Yaz, "Deterministic and stochastic robustness measures for discrete systems," *IEEE Trans. Automat. Contr.*, vol. 33, no. 10, pp. 952-955, Oct. 1988.
[9] H. J. Kushner, *Stochastic Stability and Control*. New York: Academic, 1967.
[10] R. F. Stengel, "Some effects of parameter variations on the lateral-directional stability of aircraft," *AIAA J. Guidance Contr.*, vol. 3, no. 2, pp. 124-131, Apr. 1980.
[11] ——, *Stochastic Optimal Control: Theory and Application*. New York: Wiley, 1986.
[12] R. F. Stengel and L. E. Ryan, "Stochastic robustness of linear control systems," in *Proc. 1989 Conf. Inform. Sci. Syst.*, Mar. 1989. pp. 556-561.
[13] ——, "Multivariate histograms for analysis of linear control system robustness," in *Proc. 1989 Amer. Contr. Conf.*, Pittsburgh, PA, June 1989, pp. 937-943.
[14] ——, "Application of stochastic robustness to aircraft control systems," in *Proc. 1989 AIAA Guidance, Navigation, Contr. Conf.*, Boston, MA, Aug. 1989, pp. 698-708.
[15] D. D. Siljak, *Nonlinear Systems, The Parameter Analysis and Design*. New York: Wiley, 1969.
[16] J. Ackermann, "Parameter space design of robust control systems," *IEEE Trans. Automat. Contr.*, vol. AC-25 no. 6, pp. 1058-1072, Dec. 1980.
[17] P. Putz and M. J. Wozny, "A new computer graphics approach to parameter space design of control systems," *IEEE Trans. Automat. Contr.*, vol. AC-32, no. 4, pp. 1058-1072, Apr. 1987.
[18] S. Boyd, V. Balakrishnan, C. Barratt, N. Khraishi, X. Li, D. Meyer, and S. Norman, "A new CAD method and associated architectures for linear controllers," *IEEE Trans. Automat. Contr.*, vol. 33, no. 3, pp. 268-283, Mar. 1988.
[19] W. J. Conover, *Practical Non-Parametric Statistics*. New York: Wiley, 1980.

Parallel Reduced-Order Controllers for Stochastic Linear Singularly Perturbed Discrete Systems

Zoran Gajic and Xuemin Shen

Abstract—**This note presents an approach to the decomposition and approximation of linear quadratic Gaussian control problems for singularly perturbed discrete systems at steady state. The global Kalman filter is decomposed into separate reduced-order local filters via the use of a decoupling transformation. A near-optimal control law is derived by approximating coefficients of the optimal control law. The proposed method allows parallel processing of information and reduces both off-line and on-line computational requirements. A real world example demonstrates the efficiency of the proposed method.**

Manuscript received May 22, 1989; revised October 10, 1989. Paper recommended by Past Associate Editor, M. W. Spong.

The authors are with the Department of Electrical and Computer Engineering, Rutgers University, Piscataway, NJ 08855-0909.

IEEE Log Number 9039314.

I. INTRODUCTION

Linear singularly perturbed discrete systems have been studied in a fast time-scale version [1]-[9] and slow time-scale version (e.g., [10], [11]). Discrete-time models of singularly perturbed linear systems, similar to [10], [11], were studied by Mahmoud and his co-workers [12]. Since the slow time-scale version presupposes the asymptotic stability of the fast modes, it seems, that in the design procedure of stabilizing feedback controllers, the fast time-scale version is much more appropriate [6]. In this note, we will adopt the structure of singularly perturbed discrete linear systems defined by Litkouhi and Khalil [4]-[6], and study corresponding linear-quadratic Gaussian (LQG) control problem.

The continuous-time LQG problem of singularly perturbed systems [14], [15] is solved in [16] by using the power series expansion approach, and later in [17] by using the fixed-point theory. The discrete-time LQG problem of a singularly perturbed system has not been studied, despite the extensive study of the corresponding deterministic counterpart [4]-[6]. We will resolve this problem by using results recently obtained in [18]. The main equation of the optimal linear control theory, the Riccati equation, has a quite complicated form in the discrete-time domain. Partitioning this equation, in the spirit of singular perturbation methodology, will produce a lot of terms (partitioned inversion of a matrix sum) and make the corresponding problem numerically inefficient, even though the problem order reduction is achieved. By applying a bilinear transformation [13], the solution of the discrete algebraic Riccati equation of singularly perturbed systems is obtained in [18] by using already known results for the corresponding continuous-time algebraic Riccati equation [17] (see the Appendix). The method produces the reduced-order near-optimal solution, up to an arbitrary degree of accuracy $O(\epsilon^k)$, where ϵ is a small perturbation parameter and k represents the number of iterations. This reduces the size of required off-line computations and is very suitable for parallel programming.

The importance of the existence of the $O(\epsilon^k)$ theory for singularly perturbed problems is indicated in [19], where the $O(\epsilon)$ theory fails to produce the required result, so that the existence of the $O(\epsilon^k)$ theory is a necessary requirement.

The singularly perturbed structure of the global Kalman filter is exploited in this note, such that it may be replaced by two lower order local filters which will produce additional on-line savings in required computations. This has been achieved via the use of a decoupling transformation introduced in [20], which produces the exact block diagonalization of the global Kalman filter. The approximate feedback control law is obtained by approximating coefficients of the optimal local filters with an accuracy of $O(\epsilon^N)$. The order of approximation of the optimal performance is $O(\epsilon^N)$. The order of approximation of the optimal system trajectories is $O(\epsilon^{N+1/2})$ in the case of slow variables and $O(\epsilon^N)$ in the case of fast variables. All required coefficients of desired accuracy are obtained by using the recursive reduced-order fixed-point type numerical techniques [17], [18], and [21]. Obtained numerical algorithms converge to required optimal coefficients with the rate of convergence of $O(\epsilon)$.

A real world example, a fifth-order discrete model of a steam power system [23], is included in the note, in order to demonstrate the efficiency of the proposed method.

II. LINEAR QUADRATIC GAUSSIAN CONTROL OF DISCRETE SINGULARLY PERTURBED SYSTEMS AT THE STEADY STATE

Consider the singularly perturbed discrete linear stochastic system represented in the fast time-scale by [4]-[6], [18], [25]

0018-9286/91/0100-0087$01.00